



## The challenge of non-reactive phosphorus: Mechanisms of treatment and improved recoverability using electrooxidation

Synthia Parveen Mallick<sup>a</sup>, Mohammad Shakhawat Hossain<sup>b</sup>, Arash Takshi<sup>b</sup>, Douglas F. Call<sup>c</sup>, Brooke K. Mayer<sup>a,\*</sup>

<sup>a</sup> Department of Civil, Construction and Environmental Engineering, Marquette University, 1637 West Wisconsin Avenue, Milwaukee, WI 53233, USA

<sup>b</sup> Department of Electrical Engineering, University of South Florida, 4202 East Fowler Avenue, Tampa, FL 33620, USA

<sup>c</sup> Department of Civil, Construction, and Environmental Engineering, North Carolina State University, 915 Partners Way, Raleigh, NC 27695, USA



### ARTICLE INFO

Editor: Yujie Men

**Keywords:**

Ion exchange  
Transformation  
Nutrient removal  
Wastewater  
Advanced oxidation process (AOP)  
Direct electron transfer

### ABSTRACT

Recalcitrant phosphorus (P) species, i.e., soluble non-reactive phosphorus (sNRP), are generally not effectively removed or recovered in conventional wastewater treatment processes. This was substantiated in our meta-analysis, which showed that nearly one-third of wastewater facilities' effluent P was primarily in the non-reactive form. Transformation of sNRP to more readily removable/recoverable soluble reactive phosphorus (sRP) may offer a viable pathway to enhance P removal and recovery. Electrooxidation (EO) may offer one route for sNRP to sRP transformation. During EO, different sNRP transformation pathways may occur, influencing the extent and efficiency of sNRP transformations as a function of water quality. To explore these mechanisms, we conducted oxidant quenching tests as well as cyclic voltammetry and chronoamperometry experiments using a synthetic water matrix spiked with the sNRP compound beta-glycerol phosphate (BGP). We found that direct electron transfer was responsible for BGP transformation. To assess the applicability of EO for wastewater sNRP to sRP transformation and improved recoverability, EO was used to treat municipal wastewater centrate, followed by tests of sNRP recoverability using the P-selective LayneRT™ ion exchanger. Complete transformation of centrate sNRP to sRP was not achieved with EO, but subsequent removal of sNRP using ion exchange increased after 2 hr of EO treatment. Longer periods of EO treatment did not improve sNRP removal. Improved sNRP adsorption after EO was likely due to decreased competing organics in the centrate after EO treatment. Overall, this study showed that EO can improve sNRP removal using subsequent ion exchange and facilitate enhanced P recovery.

### 1. Introduction

Excess release of nutrients, e.g., phosphorus (P), into surface waterbodies can lead to algal blooms or eutrophication, causing hypoxic conditions detrimental to aquatic life [6]. Wastewater P discharge contributes to increased P loading into surface water bodies, but advanced water reclamation processes can help minimize P discharge. Additionally, a circular P economy can be stimulated by recovering wastewater-derived P as valuable products, e.g., fertilizer and bio-fuel

feed stock. Therefore, treatment processes targeting enhanced P removal and recovery can help achieve sustainable P management. Although conventional treatment processes, e.g., enhanced biological P removal, ion exchange, chemical precipitation, filtration, coagulation, sedimentation, flocculation, and adsorption, generally remove particulate P and soluble reactive P (sRP), soluble non-reactive P (sNRP) is generally not treated effectively (see [2] and Fig. S1 in the Supporting Information [SI] for further definition of the P fractions) [22].

A recent meta-analysis of different P fractions in environmental

**Abbreviations:** BGP, Beta-glycerol phosphate; DET, Direct electron transfer; EO, Electrooxidation;  $K_F$ , Freundlich isotherm constant;  $K_L$ , Langmuir isotherm constant;  $K_{PFO}$ , Reaction constant for pseudo-first order reaction;  $K_{PSO}$ , Reaction constant for pseudo-second order reaction; MDL, Minimum detection limit; P, Phosphorus; PA, Phytic acid;  $q_e$ , Adsorption capacity at equilibrium;  $q_{max}$ , Maximum adsorption capacity; sNRP, Soluble non-reactive phosphorus; sRP, Soluble reactive phosphorus; TP, Total phosphorus.

\* Corresponding author.

E-mail addresses: [synthiaparveen.mallick@marquette.edu](mailto:synthiaparveen.mallick@marquette.edu) (S.P. Mallick), [mh666@usf.edu](mailto:mh666@usf.edu) (M.S. Hossain), [atakshi@usf.edu](mailto:atakshi@usf.edu) (A. Takshi), [dfcall@ncsu.edu](mailto:dfcall@ncsu.edu) (D.F. Call), [brooke.mayer@marquette.edu](mailto:brooke.mayer@marquette.edu) (B.K. Mayer).

<https://doi.org/10.1016/j.jece.2023.110295>

Received 11 March 2023; Received in revised form 19 May 2023; Accepted 3 June 2023

Available online 5 June 2023

2213-3437/© 2023 Elsevier Ltd. All rights reserved.

waters, municipal wastewaters, and manures included particulate P, sRP, and total P (TP) data, but the sNRP fraction was not reported [22]. While a national-scale analysis of the degree of sNRP discharge in wastewater is currently lacking, Qin et al. [19] estimated that approximately 26–81% of TP in wastewater effluent can be present in the sNRP form. Yoshimura et al. [25] reported that sNRP may comprise 5–83% of TP in the North Pacific waters, while Monbet et al. [16] found that 6–40% of total soluble P can be in the sNRP form. Given sufficient time, discharged sNRP can transform into bioavailable forms through microbial processes and cause eutrophication [19]. Due to its recalcitrance, sNRP generally cannot be recovered using conventional recovery strategies like precipitation or selective adsorption, e.g., using ion exchange. Removal of sNRP species will decrease overall eutrophication potential while its recovery will contribute to the circular P economy, an important target given the essential, yet non-renewable and non-substitutable, nature of P. Therefore, technologies targeting sNRP removal and recovery contribute to sustainable P management strategies.

Studies using UV/H<sub>2</sub>O<sub>2</sub>, UV/TiO<sub>2</sub>, Fenton, and photo-Fenton have targeted *removal* or detoxification of the parent sNRP compounds via advanced oxidation [10,3,7]. However, neither sNRP *transformation* nor subsequent *recovery* was assessed in these studies. Transformation of sNRP to sRP can provide a viable pathway for enhanced recovery as sRP is more readily recoverable through ion exchange and struvite precipitation. Transformation of sNRP to sRP is possible using electrooxidation (EO) and UV/H<sub>2</sub>O<sub>2</sub> [15,20,23]. Mallick et al. [15] reported that EO-based sNRP to sRP transformation was more effective than conventional advanced oxidation processes (AOPs), e.g., UV/H<sub>2</sub>O<sub>2</sub>, in terms of both energy efficiency and the degree of transformation. However, the energy input required for sNRP transformation to sRP was still very high, making implementation of EO for P transformation challenging [15].

The high energy demand for complete transformation of sNRP compounds may be circumvented if partial transformation of sNRP compounds can improve subsequent P recovery using adsorbents such as P-selective ion exchangers. Partially transformed sNRP compounds could potentially be concentrated using ion exchange and then further treated for enhanced removal and recovery. Therefore, this study evaluated the potential for partial transformation of sNRP using EO to improve the subsequent recoverability of sNRP species using LayneRT™ ion exchange media with the hypothesis that recovery of EO-treated sNRP compounds would be higher than untreated sNRP compounds. If LayneRT™ can remove more sNRP after EO treatment, then the high energy demand for complete sNRP transformation could be avoided.

The specific study objectives were to: (i) conduct a meta-analysis to determine the prevalence of sNRP in wastewater matrices, (ii) investigate the role of potential EO-based transformation mechanisms (e.g., oxidants sorbed on the anode surface [as in [4]], dissolved oxidants in the bulk solution, and direct electron transfer [DET]), and (iii) assess the post-EO recoverability of sNRP using ion exchange. The EO-based sNRP to sRP transformation mechanism was studied as the process can be better controlled once the dominant mechanism is identified. For instance, if DET is the dominant mechanism, then an increase in applied current density below the limiting current density would increase transformation. Lab-grade sNRP compounds were used in the mechanism analysis. To assess sNRP recoverability after EO treatment, ion exchange was used given that it can concentrate sRP to facilitate recovery of a P product suitable for direct reuse [24]. Recoverability of sNRP using ion exchange after EO was first assessed using synthetic water matrices containing phytic acid (PA) or beta-glycerol phosphate (BGP). Next, a real-world wastewater sample (centrate from an anaerobic digester) was used to assess kinetic and isotherm models of EO-treated sNRP removal using ion exchange.

## 2. Materials and methods

### 2.1. Meta-analysis to determine the prevalence of non-reactive P in wastewater

The occurrence of non-reactive P in wastewater was studied via meta-analysis. Municipal and industrial wastewater discharges for 2019 were retrieved from the U.S. Environmental Protection Agency's (EPA's) Enforcement and Compliance History Online (ECHO) website (<https://echo.epa.gov/>). The initial search returned 19,988 P data points. These data were filtered to include only those with geographically/temporally matched total and reactive P measurements, resulting in a total of 571 data points. The ECHO data did not explicitly differentiate between dissolved and particulate species.

### 2.2. Electrooxidation (EO) reactor

The EO reactor consisted of a 250-mL Berzelius beaker (holding 200 mL solution) with a 3D-printed plastic reactor cap providing 1-cm inter-electrode spacing. Titanium (Performance Titanium Group, San Diego, CA) was used as the cathode while boron-doped diamond (BDD) (Fraunhofer, Lansing, MI) was used as the anode. The surface area for each electrode was 13.5 cm<sup>2</sup>. The reactor contents were continuously stirred at 50 rpm during experiments using a multi-position magnetic stirrer (Bell-ennium, Vineland, NJ). A current density of 7.41 mA/cm<sup>2</sup> was applied using a Sorensen XPH75-2D DC Power Supply (AMETEK Inc., Berwyn, PA) for all EO experiments. The applied current density was selected based on previous experiments testing a range of current densities [15], which showed substantial sNRP transformation at 7.41 mA/cm<sup>2</sup>.

### 2.3. Investigation of the role of sorbed and dissolved oxidant mechanisms

To explore the role of sorbed versus dissolved oxidants in quencher experiments, two organic sNRP compounds previously shown to transform during EO were used: phytic acid (PA) and beta-glycerol phosphate (BGP) [15]. The initial concentration of the sNRP compounds was 1 mg P/L, consistent with the concentration used by Mallick et al. [15]. Low P concentrations were chosen as tertiary treatment may be needed to satisfy P discharge regulations, which are projected to be increasingly stringent to prevent eutrophication in receiving waterbodies.

In separate experiments, 100 mM allyl alcohol was used to quench sorbed oxidants while 100 mM tertiary butanol was used to quench dissolved oxidants. High concentrations of quenchers were used to confirm complete quenching of dissolved or sorbed oxidants. Due to the interaction between the  $\pi$ -orbital of unsaturated allyl alcohol and the anode surface, allyl alcohol primarily reacts with oxidants sorbed on the anode surface [4]. Allylic carbon is highly reactive with oxidants, and because allyl alcohol interacts very strongly with the anode surface, highly concentrated allyl alcohol (100 mM) reacts with anode-sorbed oxidants while the other compounds dissolved in the solution (here, PA or BGP) react with any dissolved oxidants generated in the system [17,5].

Tertiary butanol is a saturated alcohol that does not readily interact with the anode surface, but it does react with dissolved oxidants [12]. Therefore, tertiary butanol quenches dissolved oxidants in the bulk solution and the transformation of PA or BGP in the presence of tertiary butanol would be attributed to oxidation by sorbed oxidants.

The EO quencher tests were conducted for 30 min using 7.41 mA/cm<sup>2</sup> current density. Samples were collected at 1, 2, 5, 10, 20, and 30 min to assess the transformation kinetics of PA and BGP in the presence of allyl alcohol or tertiary butanol. All chemicals were purchased as 99% pure forms from Sigma Aldrich (St. Louis, MO). The structure of the sNRP compounds and quenchers is shown in Fig. S3.

### 2.3.1. Investigation of the role of direct electron transfer

Direct electron transfer (DET) on the anode was assessed through cyclic voltammetry and chronoamperometry tests using a VersaSTAT 4 potentiostat (Berwyn, PA). These tests were conducted in synthetic water matrices prepared by spiking deionized water with 2.6 mM sodium sulfate ( $\text{Na}_2\text{SO}_4$ ). Cyclic voltammetry experiments were conducted by scanning voltage at a rate of 50 mV/s between 0.0 V and 1.0 V. For chronoamperometry experiments, a constant voltage of 1.0 V was applied for 180 s.

Solutions were spiked with 0.2, 0.4, 1.0, 1.6, 2, 3, 4, or 8 mg P/L BGP, an sNRP compound demonstrating transformation during EO [15]. Only BGP was tested in the DET experiment as BGP and PA previously showed similar transformation trends [15]. Increasing current with increasing BGP concentration would indicate oxidation through DET.

### 2.4. Centrate characterization and treatment

After exploring the mechanisms of EO-based sNRP transformation in synthetic matrices, transformation was tested in actual wastewater matrices with high P content, i.e., centrate. Centrate was collected from the South Shore Water Reclamation Facility (Oak Creek, WI) where solids from the anaerobic digester are conditioned with Mannich polymer (Clarfloc C-321) and then thickened using a gravity belt thickener. Centrate was characterized by measuring total solids (TS), total suspended solids (TSS), volatile solids (VS), volatile suspended solids (VSS), total chemical oxygen demand (TCOD), soluble chemical oxygen demand (sCOD), dissolved organic carbon (DOC), P speciation (total P, total soluble P, total reactive P, and sRP), and UV absorbance.

The solids tests were conducted following the protocols in 2540 B, D, and E of standard methods [2]. The COD tests were conducted using the U.S. EPA-approved Hach digestion Method 8000 (Loveland, CO). After filtering samples through a 0.45  $\mu\text{m}$  PTFE syringe filter (Agela Technologies, Wilmington, DE) and acidifying them with HCl, DOC was measured using a Shimadzu TOC VCSN analyzer (Kyoto, Japan), in accordance with U.S. EPA Method 415.3. These results are compiled in Table S2.

Centrate samples were treated with 7.41 mA/cm<sup>2</sup> current density EO for 2, 4, or 6 h to achieve varying degrees of P transformation. No fouling was observed on the electrode surface after EO treatment. Mineralization of organics was determined by measuring DOC after EO treatment. Transformation of organics was further evaluated by analyzing UV absorbance after EO treatment. A UV-VIS spectroscopy scan was conducted from 200 to 400 nm using a Genesys 50 UV-VIS Spectrophotometer (Fisher Scientific, Waltham, MA) for both untreated and treated centrate samples. UV absorbance at 254 nm was recorded to assess the extent of organic transformation during EO treatment and SUVA<sub>254</sub> was calculated by normalizing DOC to UV<sub>254</sub> absorbance.

### 2.5. Ion exchange tests

LayneRT<sup>TM</sup> ion exchange resin (Layne Christensen Company, The Woodlands, TX) was used to assess the recoverability of partially transformed sNRP compounds after EO treatment. After the ion exchange experiments, total soluble P and sRP analyses were conducted (as described in Section 2.7) to determine the removal of EO-treated sNRP using ion exchange.

#### 2.5.1. Testing sNRP removal using ion exchange after EO treatment in synthetic matrices

Synthetic water matrices were prepared by spiking an electrolytic solution (600 mg/L  $\text{Na}_2\text{SO}_4$  dissolved into deionized water) with 15 mg P/L of the sNRP compound PA or BGP in separate experiments. High sNRP concentrations were used in the recoverability experiments to reflect the high P content of wastewater matrices such as centrate. The water was treated with EO for 2, 4, or 6 hr. Batch ion exchange experiments were conducted by dosing 10 mL untreated or EO-treated sNRP

solutions with 250 mg LayneRT<sup>TM</sup> to ensure the presence of sufficient ion exchanger to remove P from the bulk solution [21]. Preliminary experiments showed that no further ion exchange was achieved after 5 days (i.e., equilibrium had been achieved). Thus, samples were mixed on a Multi-Purpose Tube Rotator at 20 rpm for 5 days (Thermo Fisher Scientific, Waltham, MA).

#### 2.5.2. Kinetics of centrate sNRP removal using ion exchange

Removal of centrate sNRP using LayneRT<sup>TM</sup> was evaluated after 0, 2, 4, or 6 hr EO treatment. The kinetics of sNRP removal using ion exchange were tested by dosing 10 mL of EO-treated centrate with 250 mg LayneRT<sup>TM</sup> in independent sorption tests for 0.5, 1, 2, 3, 5, 24.5, or 48 h with constant mixing at 20 rpm on a Multi-Purpose Tube Rotator. Data points were evaluated using pseudo-first order and pseudo-second order kinetic models. The linear pseudo-first order kinetic model is shown in Eq. 1, while the linear pseudo-second order kinetic model is shown in Eq. 2.

$$\ln(q_e - q_t) = \ln q_e - K_{PFO} t \quad (1)$$

$$\frac{t}{q_t} = \frac{1}{K_{PSO}} \frac{1}{q_e^2} + \frac{1}{q_e} t \quad (2)$$

where,  $q_e$  = adsorption of sNRP at equilibrium (mg P/g LayneRT<sup>TM</sup>).

$q_t$  = adsorption capacity of sNRP at time  $t$  in hr (mg P/g LayneRT<sup>TM</sup>).

$K_{PFO}$  = pseudo-first order rate constant (1/hr).

$K_{PSO}$  = pseudo-second order rate constant (g LayneRT<sup>TM</sup>/mg P-hr).

Using the best linear model fit, nonlinear modeling was performed, as shown in Eqs. 3 and 4 for pseudo-first and pseudo-second order kinetic modeling, respectively:

$$q_t = q_e(1 - e^{-K_{PFO} t}) \quad (3)$$

$$q_t = \frac{q_e^2}{q_e} \frac{K_{PSO}}{K_{PSO}} \frac{t}{t + 1} \quad (4)$$

#### 2.5.3. Isotherm modeling of centrate sNRP removal using ion exchange

For adsorption isotherm modeling, sNRP removal using LayneRT<sup>TM</sup> ion exchange resin was tested by dosing 10 mL of centrate with 25, 50, 100, 150, 200, or 250 mg LayneRT<sup>TM</sup>. The kinetic tests of sNRP removal using LayneRT<sup>TM</sup> indicated that the change in sNRP concentration was less than 5% after 4 days. Thus, isotherm experiments were conducted for 5 days with 20 rpm mixing using a Multi-Purpose Tube Rotator. The Langmuir (Eq. 5) and Freundlich (Eq. 6) linear models were evaluated.

$$\frac{C_e}{q_e} = \frac{1}{K_L} \frac{C_e}{q_{\max}} + \frac{C_e}{q_{\max}} \quad (5)$$

$$\log q_e = \log K_F + \frac{1}{n} \log C_e \quad (6)$$

where,  $C_e$  = equilibrium concentration of sNRP (mg P/L).

$q_{\max}$  = maximum sNRP adsorption capacity (mg P/g LayneRT<sup>TM</sup>).

$K_L$  = Langmuir constant (1/mg P).

$K_F$  = Freundlich constant ([mg P/g LayneRT<sup>TM</sup>] $^n$  [L/mg P] $^{1/n}$ ).

$n$  = unitless empirical constant in the Freundlich isotherm model.

Using the best linear model fit, nonlinear modeling was performed using the Langmuir (Eq. 7) or Freundlich (Eq. 8) nonlinear isotherm models:

$$q_e = \frac{q_{\max}}{1 + K_L} \frac{C_e}{C_e} \quad (7)$$

$$q_e = K_F C_e^{1/n} \quad (8)$$

### 2.6. P analyses

Total P (TP) and reactive P measurements (after persulfate digestion,

Method 4500 P B 5) were conducted using the ascorbic acid method (4500 P E) according to standard methods [2]. Filtered samples (0.45  $\mu\text{m}$  Whatman<sup>TM</sup> cellulose membrane filter, GE Healthcare Life Sciences, Chicago, IL) were used to measure dissolved species. The concentration of sNRP was calculated by subtracting sRP from total soluble P. The minimum detection level (MDL) of the ascorbic acid method was 0.02 mg/L, calculated in accordance with the U.S. EPA recommended method [9].

### 2.7. Precipitate analysis

After EO, solid white precipitate was observed on the cathode surface (Fig. S5). The solid was analyzed using energy dispersive X-ray (EDX, JEOL JSM 6510 LV SEM, Jeol USA Inc., Peabody, MA) at 20 kV using backscattered electron imaging in the low vacuum mode. Solid precipitate was also dissolved into 5 mL 50% HCl and then analyzed using ICP-MS (7700 Series, Agilent Technologies, Santa Clara, CA) as well as via the ascorbic acid method to determine its reactive P content.

### 2.8. QA/QC and statistical analysis

All centrate characterization analyses were run in triplicate. All quenching experiments and ion exchange experiments were performed in triplicate, with results representing the average of three different centrate samples. Statistical analyses were performed in GraphPad Prism 9.3.1 (La Jolla, CA) using one-way ANOVA and Tukey post hoc analysis with a significance level of  $\alpha = 0.05$ .

## 3. Results and discussion

### 3.1. Prevalence of non-reactive P in wastewater

The highest TP loading to the 571 different receiving waterbodies in the meta-analysis was 9.6 million lb/year, with the highest non-reactive P loading at 6.8 million lb/year (Fig. 1a). The median loadings were 2239 and 546 lb/year for TP and non-reactive P, respectively. As shown in Fig. 1b, up to 100% of TP discharge can be in the non-reactive form, although the median was 33% (mean = 37.4%, n = 571). The majority of the discharged P was non-reactive in nearly one-third (32%) of the 571 facilities. Non-reactive P accounted for greater than 90% of the TP discharge in 4% of the facilities (Fig. 1c). The spatial variation of non-reactive P loading in wastewater discharge is shown by state in Fig. S2.

As shown in Fig. 1, a substantial fraction of the wastewater effluent TP can be in non-reactive forms. When released into environmental waters, the non-reactive forms can cause eutrophication either via direct bio-assimilation or after enzymatic transformation to sRP [19]. Therefore, to decrease TP discharge and reduce the negative effects of excessive P levels in environmental waters, wastewater treatment targeting reduction of sNRP as part of TP management is critical (for example, transforming sNRP using EO followed by removal using ion exchange).

### 3.2. The role of sorbed and dissolved oxidants in electrooxidation (EO)-based P transformation

Oxidative transformation of sNRP during EO could occur through three potential pathways: 1) reactions with oxidants sorbed on the electrode surface [4], 2) reactions with oxidants in the bulk solution,

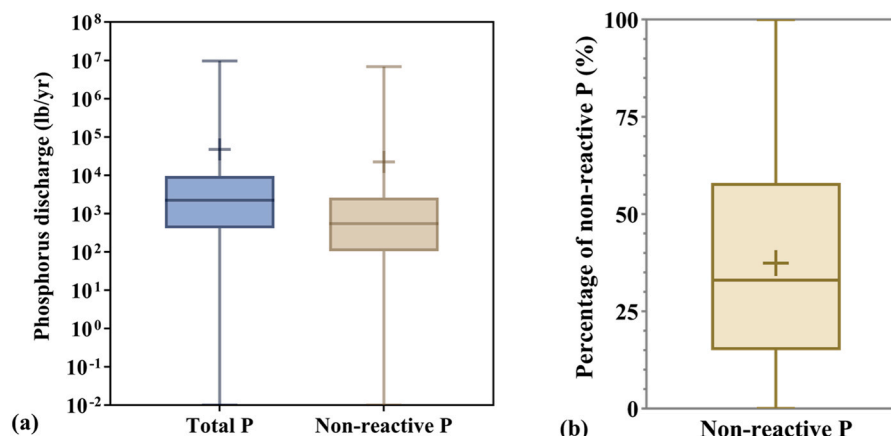
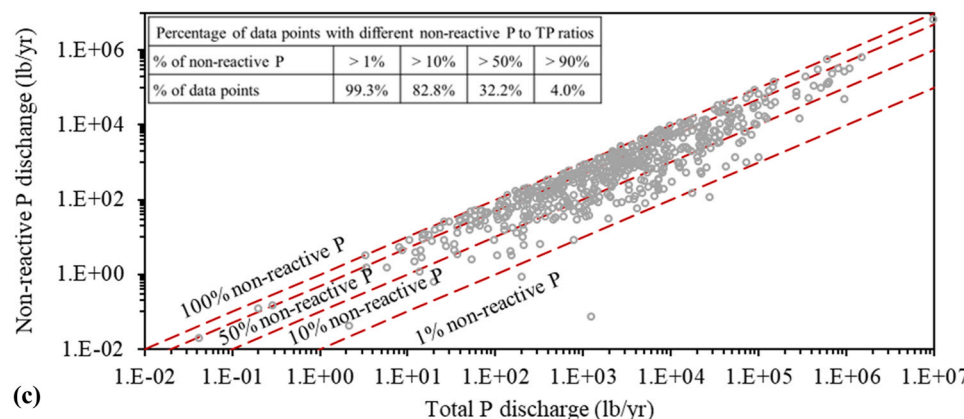


**Fig. 1.** Variability of (a) total phosphorus (TP) and non-reactive P loading and (b) percentage of non-reactive P in wastewater effluent TP discharge. The whiskers represent the minimum and maximum values in the data set, the boxes represent the 25th and 75th percentile values with a median line inside the box, and the mean is shown as a “+” sign. (c) Non-reactive P versus TP loading in wastewater effluent. Data for wastewater effluent ( $n = 571$  from 571 sites) was from the Enforcement and Compliance History Online (ECHO) website for the U.S. in 2019.



and 3) DET. Quenching experiments were performed to systematically assess the relative role of each of these mechanisms. Transformation of the sNRP compounds PA and BGP by EO in the presence of allyl alcohol and tertiary butanol quenchers was significantly less compared to transformation without any quencher ( $p < 0.0001$ ) (Fig. 2a). Low transformation in the presence of both quenchers indicated that neither sorbed nor dissolved oxidants played a critical role in the transformation of sNRP compounds. While DET transformation of PA or BGP should still occur in the presence of either quencher, the low levels of transformation observed are believed to be a result of the relatively high concentration of quenchers used (100 mM) compared to the orders of magnitude lower concentrations of PA (5.4  $\mu$ M or 1 mg P/L) and BGP (32.3  $\mu$ M or 1 mg P/L) in solution. The highly concentrated quenchers likely outcompeted PA or BGP for DET, resulting in low sNRP transformation.

Transformation of PA and BGP followed zero order kinetics in the presence of the quenchers (Fig. 2b), consistent with PA and BGP transformation without quenching, as reported by [15]. Zero order kinetics are expected to prevail when DET is the dominant mechanism in the electrochemical reactor [1]. The rate constants corresponding to PA and BGP transformation with quenchers were statistically similar ( $p \geq 0.1572$ , Table S1).

### 3.3. Confirmation of direct electron transfer (DET) for P transformation

As discussed in the previous section, EO-based sNRP to sRP transformation was likely achieved due to DET. However, the quencher experiments did not directly assess DET of sNRP compounds. Therefore, cyclic voltammetry and chronoamperometry experiments were conducted using BGP to assess DET. There was no detectable peak in the cyclic voltammetry diagram (Fig. S4), likely because EO-based sNRP transformation at low applied current density is not limited by mass transfer. The chronoamperometry experiments showed that with increased BGP concentration, the steady state current increased linearly

(Fig. 3). An increase in the steady state current with a relatively high concentration of BGP in solution indicated that BGP caused additional electron transfer, or DET.

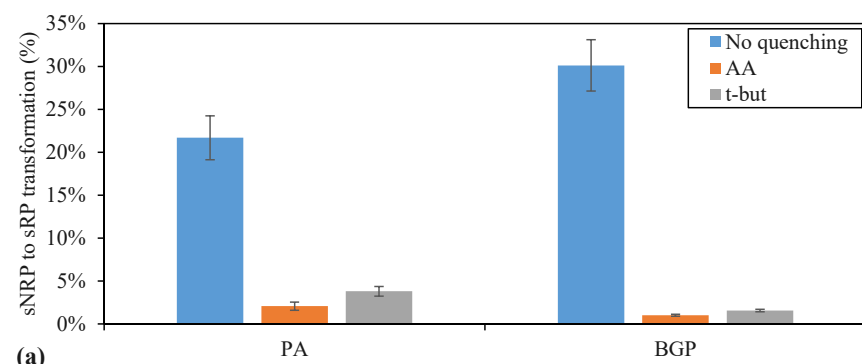
The cumulative evidence of low transformation in the presence of oxidant quenchers, zero order kinetics, cyclic voltammetry, and chronoamperometry experiments indicated that DET was the dominant mechanism in EO-based sNRP transformation. This information is important to inform process control and electrode design. For instance, since DET is the dominant mechanism in EO-based transformation, higher transformation can be achieved by applying higher current density. Higher surface area electrodes may also be used to increase volumetric transformation rates.

### 3.4. Removal of sNRP after EO treatment using ion exchange: Synthetic water matrices

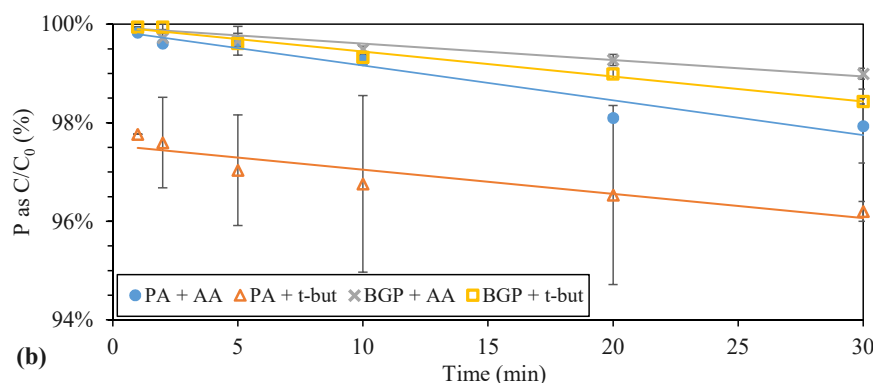
After EO treatment, sNRP removal using ion exchange in synthetic water matrices containing PA or BGP improved significantly with each incremental increase in EO treatment ( $p < 0.0001$ , Fig. 4). Compared to synthetic matrices without EO treatment, 11% more sNRP removal was achieved using 6-hr of EO followed by ion exchange. Increased sNRP removal using LayneRT™ after EO treatment indicated that partial transformation of sNRP compounds increased removal using ion exchange.

### 3.5. Shifts in centrate P speciation after EO

In realistic water matrices, the presence of organics and other constituents could compete with sNRP transformation. Therefore, removal of EO-treated sNRP in centrate using ion exchange was tested. The centrate was first treated with EO for 2, 4, or 6 hr. Complete transformation of wastewater centrate sNRP (as indicated by an increase in reactive P species) was not observed after EO treatment (Fig. 5). However, TP and total reactive P decreased significantly ( $p \leq 0.0058$ ) after



**Fig. 2. (a)** Electrooxidation (EO)-based transformation of phytic acid (PA) and beta-glycerol phosphate (BGP) in 600 mg/L  $\text{Na}_2\text{SO}_4$  electrolyte with and without the addition of 100 mM allyl alcohol (AA) or tertiary butanol (t-but) quenchers under neutral pH condition after 30 min of EO treatment conducted at 7.41 mA/cm<sup>2</sup> current density and 50 rpm mixing speed. **(b)** Transformation kinetics for PA and BGP in the presence of AA and t-but quenchers under the same EO treatment conditions. Data points show the average of triplicate experiments, and the error bars represent  $\pm 1$  standard error.



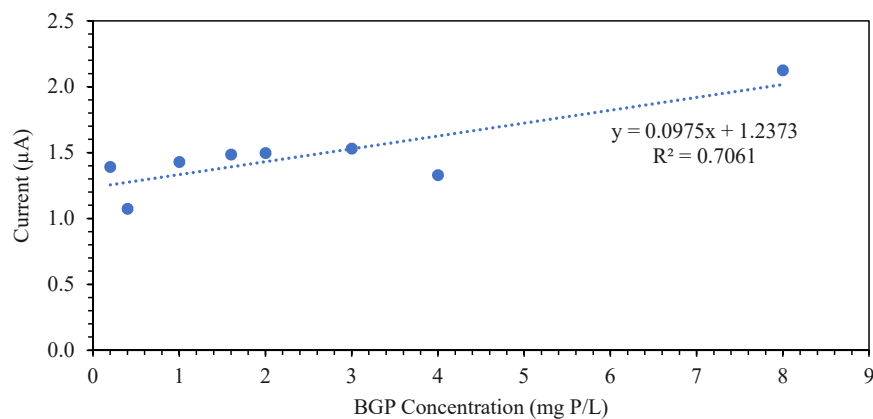


**Fig. 3.** Steady state current in chronoamperometry tests versus BGP concentration. Experiments were conducted at varying BGP concentrations (0.2, 0.4, 1.0, 1.6, 2, 3, 4, and 8 mg P/L). An increase in the steady state current with higher BGP concentrations indicated that additional electron transfer occurred when more BGP was added, confirming DET as the mechanism for BGP transformation in the electrooxidation reactor. Each data point corresponds to a single chronoamperometry experiment.

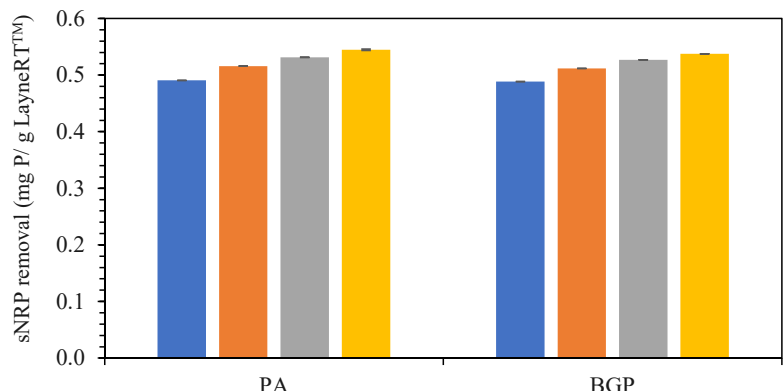


**Fig. 4.** Removal of soluble non-reactive phosphorus (sNRP) using LayneRT™ after electrooxidation (EO) treatment in electrolytic (600 mg/L Na<sub>2</sub>SO<sub>4</sub>) synthetic water matrices containing either phytic acid (PA) or beta-glycerol phosphate (BGP). EO was performed using 7.41 mA/cm<sup>2</sup> current density and 50 rpm mixing speed for 0, 2, 4, or 6 hr. The ion exchange experiments were conducted for 5 days in batch experiments at 20 rpm mixing speed dosing 10 mL of synthetic water matrices (15 mg P/L) with 250 mg LayneRT™. The bars in the figure represent averages of triplicate analyses while the error bars represent  $\pm 1$  standard error.

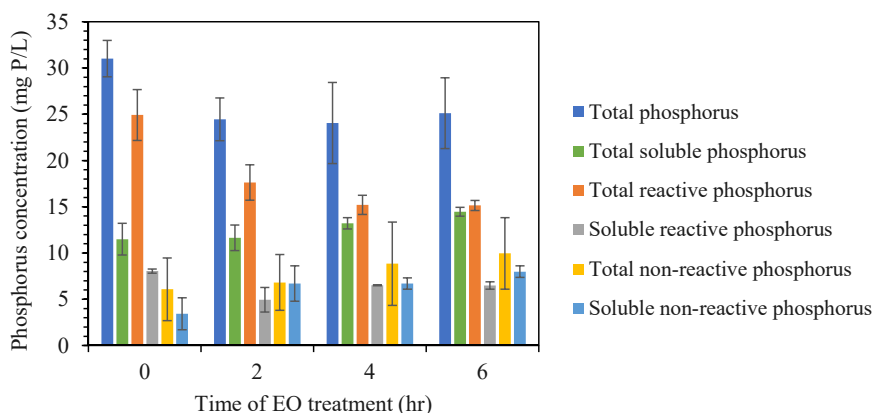


**Fig. 5.** Phosphorus (P) speciation in municipal wastewater centrate before and after electrooxidation (EO). EO was performed using 7.41 mA/cm<sup>2</sup> current density and 50 rpm mixing speed. The bars represent averages of triplicate analyses while the error bars represent  $\pm 1$  standard error.

2 hr of EO treatment, with no further decreases after 4 and 6 hr of EO treatment ( $p \geq 0.5584$ ). Given that there was no significant change in total soluble P, sRP, or sNRP before and after treatment ( $p \geq 0.147$ ), the decrease in TP and total reactive P was attributed to transformation to particulate reactive P, which partitioned out of solution, as observed by the deposition of a white precipitate on the titanium cathode surface after EO treatment (Fig. S5).

The EDX analysis of the solids showed peaks for magnesium, calcium, phosphorus, oxygen, and carbon (Fig. S6), indicating that the precipitate might contain phosphates of magnesium and calcium. Further ICP-MS analysis of the precipitate showed it contained 1.2 mg (38  $\mu$ mol) P. The summation of reactive P in the precipitate and bulk

solution was statistically similar to the bulk solution reactive P content in the untreated centrate (Fig. S7,  $p = 0.7730$ ). ICP-MS analysis showed that the precipitate contained 1.5 mg (62  $\mu$ mol) magnesium and 5.2 mg (131  $\mu$ mol) calcium, indicating that the precipitate could be a mix of calcium and magnesium phosphates. The bulk solution pH remained at 8.2 – 8.4 throughout EO treatment. This slightly alkaline pH is generally not suitable for magnesium or calcium phosphate precipitation [8]. However, the local pH at the titanium cathodes can be much higher (9.9 – 14.5), facilitating precipitation on the electrode surface [11].

Although no transformation to sRP was achieved, mineralization of organic carbon was observed during EO treatment, confirming EO process performance (Section S7 of the SI). The lack of P transformation and

low level of carbon mineralization indicate that not all energy input into the system was directed toward transforming the organics in solution; instead, energy was lost in the process. The EO reactor configuration (BDD anode and titanium cathode) does not have any selectivity towards P compounds, and an array of additional reactions, e.g., hydrogen or oxygen evolution and intermediate generation, may have occurred. Such reactions could consume energy, detracting from sNRP transformation. Moreover, compared to sNRP transformation in synthetic water matrices [15], the C/P ratio is much higher in centrate (3.6 in centrate vs. 0.4 in PA and 1.16 in BGP), which might also negatively affect P transformation in centrate.

### 3.6. Removal of EO-treated centrate P using ion exchange: Kinetics and isotherms

A major goal of this study was to assess if EO treatment could increase the recoverability of centrate sNRP such that improved removal of partially transformed sNRP after EO would circumvent the high energy demand of complete transformation to sRP (the P form most amenable to removal and recovery). As shown by the kinetic (Fig. 6) and isotherm (Fig. 7) modeling using LayneRT<sup>TM</sup> ion exchange resin, EO treatment improved removal of centrate sNRP species without the need for complete transformation to sRP.

The pseudo-second order linear kinetic model of sNRP removal using LayneRT<sup>TM</sup> offered a strong fit ( $R^2 \geq 0.78$ , as shown in Fig. S10b; the non-linear model is shown in Fig. 6) indicating that sNRP removal using LayneRT<sup>TM</sup> depended on the diffusion of sNRP to the ion exchange sites [18].

There was a significant increase in sNRP removal capacity ( $q_e$ ) between the untreated centrate sample ( $t = 0$ ) and after 2 hr of EO treatment ( $p = 0.0061$ ) (Fig. 6). Subsequent incremental increases in EO treatment time did not significantly improve adsorption capacity ( $p \geq 0.0920$ ). This demonstrates that even though EO did not completely transform sNRP compounds (Fig. 5), the compounds were still more easily removable and recoverable using ion exchange after EO.

The linear Langmuir model provided a better fit ( $R^2 \geq 0.85$ ) for sNRP removal using LayneRT<sup>TM</sup> than the Freundlich model ( $R^2 \leq 0.07$ ) (Fig. S11). The non-linear Langmuir model is thus shown in Fig. 7. The maximum sNRP removal capacity ( $q_{max}$ ) increased significantly after 2 hr of EO treatment ( $p = 0.0141$ ). However, further improvement in  $q_{max}$  was not achieved after 4 and 6 hr of EO treatment ( $p \geq 0.7146$ ). LayneRT<sup>TM</sup>'s affinity for sNRP adsorption, represented by the Langmuir constant ( $K_J$ ), did not change significantly after EO treatment ( $p \geq 0.8069$ ). Given that complete sNRP transformation was not observed (Fig. 5) and that partial transformation of sNRP would be anticipated to improve sorption capacity (Fig. 4), this lack of change in affinity suggests that negligible sNRP transformation occurred. However, the wastewater organic analysis showed that after EO treatment, there were fewer organics (particularly aromatic organics, as

represented by SUVA<sub>254</sub>), such that sNRP had less competition for the ion exchange sites [21].

### 3.7. Recommendations for future work

While EO treatment improved sNRP removal using ion exchange, the energy input to do so was generally high. In this study, the energy consumption for centrate sNRP transformation using EO could not be calculated as complete transformation was not achieved. However, Mallick et al. [15] previously reported that sNRP transformation in synthetic water matrices consumed  $10^7$  kWh/kg energy using EO. The energy input is likely to be even higher for centrate sNRP transformation. Quantification of the energy losses e.g., through hydrogen or oxygen evolution reactions, formation of intermediates, and/or system resistance due to double layer capacitance on the anode surface, will inform future improvements in the energy efficiency of EO-based nutrient transformation.

Given that DET was the dominant mechanism in EO-based sNRP transformation, increasing electrode surface area may improve transformation. However, increasing surface area would also add to operating costs. Moreover, depending on the electrode material, the kinetics of sNRP transformation may change. Future research into EO reactor configuration (electrode materials and surface area of electrode) is needed to develop better understanding of EO-based nutrient transformation process efficiency.

## 4. Conclusions

The meta-analysis presented in this study showed that sNRP can comprise a substantial fraction of TP discharge from wastewater. The majority of the TP load was in the non-reactive form in 32% of the facilities. Although sNRP species are recalcitrant and less bioavailable compared to sRP, they can still cause eutrophication. Therefore, sNRP discharge into receiving waterbodies needs to be controlled.

Transformation of sNRP into more readily removable/recoverable species using EO (the dominant mechanism for which is DET) can facilitate sNRP recovery from wastewater. Removal of sNRP compounds in synthetic water matrices using ion exchange improved significantly after EO treatment. However, when EO was used to treat centrate, complete transformation of sNRP was not achieved. Reactive P from the bulk solution precipitated as particulate P (ostensibly magnesium and calcium phosphates) on the cathode surface, potentially offering a P recovery pathway if the precipitate is separated for reuse applications, e.g., as fertilizer. Although centrate sNRP did not completely transform, recoverability of the EO-treated centrate sNRP increased. Since the affinity for sNRP removal using LayneRT<sup>TM</sup> ion exchanger was virtually the same before and after EO treatment, increased removal of sNRP after EO treatment can likely be attributed to less competition from organics in the EO-treated centrate samples. However, increasing recoverability

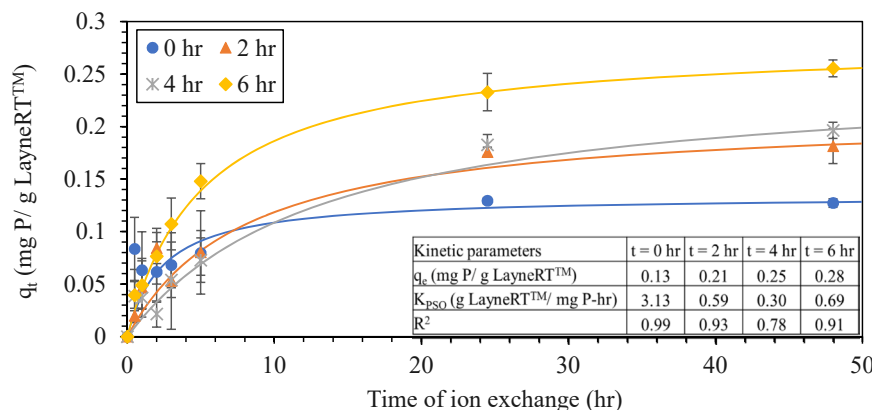


**Fig. 6.** Pseudo-second order non-linear kinetic models of soluble non-reactive P (sNRP) removal from wastewater centrate using LayneRT<sup>TM</sup> ion exchange resin after electrooxidation (EO) treatment for 0, 2, 4, or 6 hr. EO was operated at  $7.41 \text{ mA/cm}^2$  current density and 50 rpm mixing speed. The ion exchange kinetics were conducted in batch experiments at 20 rpm mixing speed dosing 10 mL of centrate with 250 mg LayneRT<sup>TM</sup>. The points represent averages of triplicate analyses while the error bars represent  $\pm 1$  standard deviation.

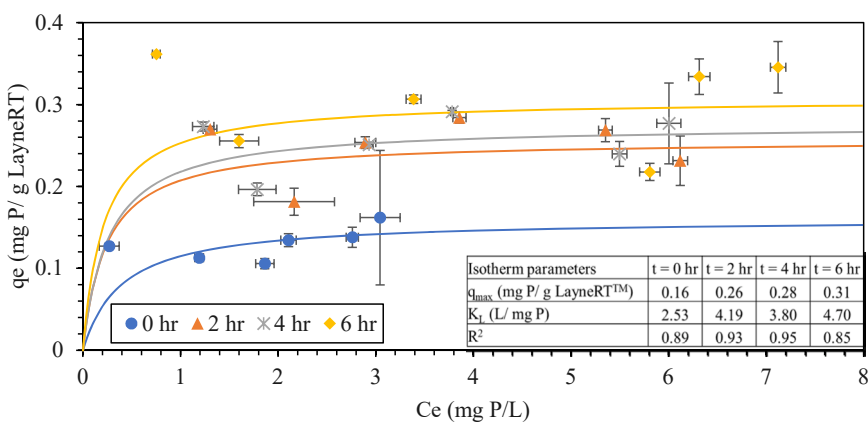


**Fig. 7.** Langmuir isotherm of soluble non-reactive phosphorus (sNRP) removal using LayneRT™ ion exchange material after electrooxidation (EO) treatment for 2, 4, or 6 hr. EO was operated at  $7.41 \text{ mA/cm}^2$  current density and 50 rpm mixing speed. Isotherms were conducted in batch experiments at 20 rpm mixing speed for 5 days, which was sufficient to achieve equilibrium. The points represent averages of triplicate analyses while the error bars represent  $\pm 1$  standard deviation.

of centrate sNRP using EO might not be a practical choice due to the low increase in recoverability in response to the high energy input. Alternate pathways, e.g., selective adsorption [14,13], may offer a more efficient means of improved sNRP removal and recovery from wastewater.

#### CRediT authorship contribution statement

**Synthia Parveen Mallick:** Conceptualization, Methodology, Validation, Formal analysis, Investigation, Data curation, Writing – original draft, Writing – review & editing, Visualization. **Mohammad Shakhat Hossain:** Methodology, Validation, Formal analysis, Investigation, Writing – review & editing. **Arash Takshi:** Methodology, Resources, Writing – review & editing, Supervision, Project administration. **Douglas F. Call:** Conceptualization, Writing – review & editing, Project administration, Funding acquisition. **Brooke K. Mayer:** Conceptualization, Resources, Writing – review & editing, Supervision, Project administration, Funding acquisition.

#### Declaration of Competing Interest

The authors declare the following financial interests/personal relationships which may be considered as potential competing interests: Brooke Mayer, Synthia Mallick, and Douglas Call report financial support was provided by the National Science Foundation.

#### Data Availability

Data will be made available on request.

#### Acknowledgments

This project was supported by the Science and Technologies for Phosphorus Sustainability (STEPS) Center under National Science Foundation (NSF) award number CBET-2019435. All conclusions are those of the authors and do not necessarily reflect the views of the NSF. We sincerely thank Mike Dollhopf and Jonathon Hou for their assistance with COD and  $\text{NH}_3$  analyses. We also thank Dr. Raymond Fournelle for his assistance with the EDX analysis.

#### Appendix A. Supporting information

Supplementary data associated with this article can be found in the online version at [doi:10.1016/j.jece.2023.110295](https://doi.org/10.1016/j.jece.2023.110295).

#### References

- [1] F. Almomani, R. Bhosale, M. Khrasheh, A. Kumar, M. Tawalbeh, Electrochemical oxidation of ammonia on nickel oxide nanoparticles, *Int. J. Hydrol. Energy* 45 (2020) 10398–10408, <https://doi.org/10.1016/J.IJHYDENE.2019.11.071>.
- [2] APHA, 2012. Standard methods for the examination of water and wastewater, 22nd ed. American Public Health Association, American Water Works Association, Water Environment Federation, Washington D.C., USA.
- [3] M.I. Badawy, M.Y. Ghaly, T.A. Gad-Allah, Advanced oxidation processes for the removal of organophosphorus pesticides from wastewater, *Desalination* 194 (2006) 166–175, <https://doi.org/10.1016/j.desal.2005.09.027>.
- [4] J.M. Barazesh, C. Prasse, D.L. Sedlak, Electrochemical transformation of trace organic contaminants in the presence of halide and carbonate ions, *Environ. Sci. Technol.* 50 (2016) 10143–10152, <https://doi.org/10.1021/acs.est.6b02232>.
- [5] R. Celdrán, J.J. González-Velasco, Oxidation mechanism of allyl alcohol on an Au-electrode in basic solutions, *Electrochim. Acta* 26 (1981) 525–533, [https://doi.org/10.1016/0013-4686\(81\)87033-8](https://doi.org/10.1016/0013-4686(81)87033-8).
- [6] D.J. Conley, H.W. PAERL, R.W. Howarth, D.F. Boesch, S.P. Seitzinger, K.E. Havens, Controlling eutrophication: nitrogen and phosphorus, *Science* 323 (2009) 1014–1015, <https://doi.org/10.1126/science.1167755>.
- [7] N. Daneshvar, M.J. Hejazi, B. Rangarangy, A.R. Khataee, Photocatalytic degradation of an organophosphorus pesticide phosalone in aqueous suspensions of titanium dioxide, *J. Environ. Sci. Health - Part B Pestic., Food Contam., Agric. Wastes* 39 (2004) 285–296, <https://doi.org/10.1081/PCF-120030242>.
- [8] O.A. Diaz, K.R. Reddy, P.A. Moore, Solubility of inorganic phosphorus in stream water as influenced by pH and calcium concentration, *Water Res.* 28 (1994) 1755–1763, [https://doi.org/10.1016/0043-1354\(94\)90248-8](https://doi.org/10.1016/0043-1354(94)90248-8).
- [9] EPA, 2016. Definition and Procedure for the Determination of the Method Detection Limit, Revision 2. Washington D.C.
- [10] H.E. Gray, T. Powell, S. Choi, D.S. Smith, W.J. Parker, Organic phosphorus removal using an integrated advanced oxidation-ultrafiltration process, *Water Res.* 182 (2020), 115968, <https://doi.org/10.1016/J.WATRES.2020.115968>.
- [11] Y. Lei, B. Song, R.D. van der Weijden, M. Saakes, C.J.N. Buisman, Electrochemical induced calcium phosphate precipitation: importance of local pH, *Environ. Sci. Technol.* 51 (2017) 11156–11164, <https://doi.org/10.1021/acs.est.7b03909>.
- [12] A. Malliaris, J. Lang, R. Zana, Kinetics and mechanism of the oxidation of allyl alcohol on Ag(110), *J. Phys. Chem.* 91 (1987) 655.
- [13] S.P. Mallick, Z. Mallick, B.K. Mayer, Meta-analysis of the prevalence of dissolved organic nitrogen (DON) in water and wastewater and review of DON removal and recovery strategies, *Sci. Total Environ.* 828 (2022), 154476, <https://doi.org/10.1016/J.SCITOTENV.2022.154476>.
- [14] S.P. Mallick, F.B. Hussein, S. Husted, B.K. Mayer, Adsorption of recalcitrant phosphorus compounds using the phosphate-selective binding-protein PstS, *Chemosphere* 304 (2022), 135311, <https://doi.org/10.1016/j.chemosphere.2022.135311>.
- [15] S.P. Mallick, D.R. Ryan, K. Venkiteshwaran, P.J. McNamara, B.K. Mayer, Electro-oxidation to convert dissolved organic nitrogen and soluble non-reactive phosphorus to more readily removable and recoverable forms, *Chemosphere* (2021) 279, <https://doi.org/10.1016/j.chemosphere.2021.130876>.
- [16] P. Monbet, I.D. McKelvie, P.J. Worsfold, Dissolved organic phosphorus speciation in the waters of the Tamar estuary (SW England), *Geochimica et Cosmochimica Acta* 73 (2009) 1027–1038, <https://doi.org/10.1016/j.gca.2008.11.024>.
- [17] E. Pastor, V.M. Schmidt, T. Iwasita, M.C. Arévalo, S. González, A.J. Arvia, The reactivity of primary C3-alcohols on gold electrodes in acid media. A comparative study based on dems data, *Electrochim. Acta* 38 (1993) 1337–1344, [https://doi.org/10.1016/0013-4686\(93\)80067-A](https://doi.org/10.1016/0013-4686(93)80067-A).
- [18] W. Plazinski, J. Dziuba, W. Rudzinski, Modeling of sorption kinetics: the pseudo-second order equation and the sorbate intraparticle diffusivity, *Adsorption* 19 (2013) 1055–1064, <https://doi.org/10.1007/S10450-013-9529-0/FIGURES/5>.

[19] C. Qin, H. Liu, L. Liu, S. Smith, D.L. Sedlak, A.Z. Gu, Bioavailability and characterization of dissolved organic nitrogen and dissolved organic phosphorus in wastewater effluents, *Sci. Total Environ.* 511 (2015) 47–53, <https://doi.org/10.1016/j.scitotenv.2014.11.005>.

[20] H.R. Sindelar, J. Lloyd, M.T. Brown, T.H. Boyer, Transformation of dissolved organic phosphorus to phosphate using UV/H<sub>2</sub>O<sub>2</sub>, *Environ. Prog. Sustain. Energy* 35 (2016) 680–691, <https://doi.org/10.1002/ep.12272>.

[21] Y. Tong, P.J. McNamara, B.K. Mayer, Fate and impacts of triclosan, sulfamethoxazole, and 17 $\beta$ -estradiol during nutrient recovery via ion exchange and struvite precipitation, *Environ. Sci.: Water Res. Technol.* 3 (2017) 1109–1119, <https://doi.org/10.1039/C7EW00280G>.

[22] K. Venkiteswaran, P.J. McNamara, B.K. Mayer, Meta-analysis of non-reactive phosphorus in water, wastewater, and sludge, and strategies to convert it for enhanced phosphorus removal and recovery, *Sci. Total Environ.* (2018), <https://doi.org/10.1016/j.scitotenv.2018.06.369>.

[23] K. Venkiteswaran, E. Kennedy, C. Graeber, S.P. Mallick, P.J. McNamara, B. K. Mayer, Conversion of soluble recalcitrant phosphorus to recoverable orthophosphate form using UV/H<sub>2</sub>O<sub>2</sub>, *Chemosphere* (2021) 278, <https://doi.org/10.1016/j.chemosphere.2021.130391>.

[24] A.T. Williams, D.H. Zitomer, B.K. Mayer, Ion exchange-precipitation for nutrient recovery from dilute wastewaters, *Environ. Sci.: Water Res. Technol.* 1 (2016) 832–838, <https://doi.org/10.1039/c5ew00142k>.

[25] T. Yoshimura, J. Nishioka, H. Saito, S. Takeda, A. Tsuda, M.L. Wells, Distributions of particulate and dissolved organic and inorganic phosphorus in North Pacific surface waters, *Marine Chemistry* 103 (2007) 112–121, <https://doi.org/10.1016/j.marchem.2006.06.011>.